

Vertical profiles of lightning-produced NO₂ enhancements in the upper troposphere observed by OSIRIS

C. E. Sioris^{1,2,3}, C. A. McLinden¹, R. V. Martin^{3,4}, B. Sauvage⁴, C. S. Haley⁵, N. D. Lloyd², E. J. Llewellyn², P. F. Bernath^{6,7}, C. D. Boone⁶, S. Brohede⁸, and C. T. McElroy¹

¹Experimental Studies Section, Environment Canada, Toronto, ON, Canada

²Institute of Space and Atmospheric Studies, University of Saskatchewan, Saskatoon, SK, Canada

³Atomic and Molecular Physics Division, Harvard-Smithsonian Center for Astrophysics, Cambridge, MA, USA

⁴Department of Physics and Atmospheric Science, Dalhousie University, Halifax, NS, Canada

⁵Department of Physics and Atmospheric Science, Dalhousie University, Centre for Research in Earth and Space Science, York University, Toronto, Ontario, Canada

⁶Department of Chemistry, University of Waterloo, Waterloo, ON, Canada

⁷Department of Chemistry, University of York, Heslington, York, UK

⁸Department of Radio and Space Science, Chalmers University of Technology, Göteborg, Sweden

Received: 27 February 2007 – Published in Atmos. Chem. Phys. Discuss.: 11 April 2007

Revised: 16 August 2007 – Accepted: 16 August 2007 – Published: 21 August 2007

Abstract. The purpose of this study is to perform a global search of the upper troposphere ($z \geq 10$ km) for enhancements of nitrogen dioxide and determine their sources. This is the first application of satellite-based limb scattering to study upper tropospheric NO₂. We have searched two years (May 2003–May 2005) of OSIRIS (Optical Spectrograph and Infrared Imager System) operational NO₂ concentrations (version 2.3/2.4) to find large enhancements in the observations by comparing with photochemical box model calculations and by identifying local maxima in NO₂ volume mixing ratio. We find that lightning is the main production mechanism responsible for the large enhancements in OSIRIS NO₂ observations as expected. Similar patterns in the abundances and spatial distribution of the NO₂ enhancements are obtained by perturbing the lightning within the GEOS-Chem 3-dimensional chemical transport model. In most cases, the presence of lightning is confirmed with coincident imagery from LIS (Lightning Imaging Sensor) and the spatial extent of the NO₂ enhancement is mapped using nadir observations of tropospheric NO₂ at high spatial resolution from SCIAMACHY (Scanning Imaging Absorption Spectrometer for Atmospheric Chartography) and OMI (Ozone Monitoring Instrument). The combination of the lightning and chemical sensors allows us to investigate globally the role of lightning to the abundance of NO₂ in the upper troposphere (UT). Lightning contributes 60% of the tropical upper tropospheric NO₂ in GEOS-Chem simulations. The spatial and temporal distribution of NO₂ enhancements from lightning (May

2003–May 2005) is investigated. The enhancements generally occur at 12 to 13 km more frequently than at 10 to 11 km. This is consistent with the notion that most of the NO₂ is forming and persisting near the cloud top altitude in the tropical upper troposphere. The latitudinal distribution is mostly as expected. In general, the thunderstorms exhibiting weaker vertical development (e.g. $11 \leq z \leq 13$ km) extend latitudinally as far poleward as 45° but the thunderstorms with stronger vertical development ($z \geq 14$ km) tend to be located within 33° of the equator. There is also the expected hemispheric asymmetry in the frequency of the NO₂ enhancements, as most were observed in the northern hemisphere for the period analyzed.

1 Introduction

Lightning generates most of the NO_x (NO₂ and NO) in the low latitude upper troposphere (Lamarque et al., 1996) and has important consequences for atmospheric chemistry and climate (WMO, 1999; Intergovernmental Panel on Climate Change, 2001). However, considerable uncertainty remains in the magnitude of this natural source of NO_x (e.g. Price et al., 1997; Nesbitt et al., 2000; Schumann and Huntrieser, 2007). The vertical distribution of the lightning NO_x emissions also requires further study.

Of the available remote sensing techniques to observe lightning-generated NO₂ in the upper troposphere on a global scale, limb scattering is uniquely suited. Limb scattering has a tremendous advantage over solar occultation in terms of data volume and spatial coverage because the latter technique

Correspondence to: C. E. Sioris
(christopher.sioris@ec.gc.ca)

is limited to measuring only when the sun is on the horizon and in the field of view. Limb scattering provides the opportunity for profile information at high vertical resolution with global coverage (Haley et al., 2004). Infrared emission techniques also provide global coverage and can measure at night as well, however the only limb-viewing infrared emission instrument currently available, measures profiles of NO₂ with a vertical resolution of 9–12 km below 16 km (Funke et al., 2004). The space borne limb scattering instruments currently capable of providing upper tropospheric NO₂ profile information are SCIAMACHY (Scanning Imaging Absorption Spectrometer for Atmospheric Chartography) (Bovensmann et al., 1999) and OSIRIS (Optical Spectrograph and Infrared Imager System) (Llewellyn et al., 2004). SCIAMACHY can measure NO₂ profiles down to the upper troposphere at low latitudes with an effective vertical resolution of ~3.3 km, dictated by coarse vertical sampling and large instantaneous field of view (2.6 km high by 110 km wide at the tangent point). OSIRIS yields NO₂ profiles with a typical vertical resolution of ~2 km (full width at half-maximum of the averaging kernel for the retrieval technique used below) at the median altitude of the observed NO₂ enhancements of 13 km.

The spectrograph of OSIRIS measures limb scattered radiation in the 280–810 nm range with ~1 nm spectral resolution. The instantaneous field of view is 1 km × 30 km (vertical, horizontal) at the tangent point, allowing OSIRIS to see through partly cloudy scenes more effectively and providing better vertical resolution than SCIAMACHY, and is ideal for global studies of vertically-structured phenomena such as NO₂ enhancements from lightning. Odin, the satellite bearing OSIRIS, has a polar sun-synchronous orbit with equator crossing times of 06:00 and 18:00 LT. SCIAMACHY, on the other hand, measures only at ~10:15 LT. One of the advantages of the equator crossing times of the Odin orbit is that OSIRIS can observe approximately the same volume of air in the summer hemisphere within 12 h. This advantage is exploited in this study. The related disadvantage is that OSIRIS gets poor coverage in the winter hemisphere. However, since most of the lightning occurs in the summer hemisphere, the orbit is well suited. Furthermore, with observational local times near twilight, NO_x partitioning is more balanced between NO₂ and NO in the tropical upper troposphere, leading to stronger NO₂ absorption signals compared to midday.

In this paper, we reveal the magnitude and spatial and temporal distribution of the observed enhancements and then highlight some interesting case studies.

2 Data analysis method

We start with operationally-retrieved version 2.3/2.4 NO₂ profiles. The retrieval method for the operational NO₂ product is described in detail by Haley et al. (2004). The version 3.0 (v3.0) operational data product contains a significant im-

provement: the retrievals only extend down to cloud top, if present. However, the operational algorithm for determining cloud tops, occasionally misidentifies the upper end of the stratospheric aerosol layer in the tropics as being a cloud top and thus a significant fraction of tropical upper tropospheric data is lost. Thus we use v2.3/2.4 data (available only to May 2005) and an offline cloud top product described below to filter cloudy cases.

The operationally-retrieved profiles are compared with profiles generated by a stacked photochemical box model (McLinden et al., 2000) for the same local time, month, and latitude. The model extends down to ~10 km at all latitudes, and thus it covers the retrieval range of operational OSIRIS NO₂ (i.e. 10 to 46 km) with comparable vertical resolution (~2 km). When

1. the observed profile exceeds the model profile by 1 order of magnitude at any altitude, or
2. the observed volume mixing ratio (VMR) at a given altitude minus its 1σ uncertainty is greater than the VMR plus the 1σ uncertainty for the immediately overlying layer,

the limb scan is selected and the data are reanalyzed using the algorithm described previously (Sioris et al., 2003; Sioris et al., 2004), with modifications detailed below.

The first step of this retrieval algorithm is to check for the presence of clouds using the ~810 nm limb radiance profile. Five spectral pixels are co-added to reduce the impact of spikes in the data, which result mostly when the satellite is in the region of the south Atlantic anomaly (Heitzler, 2002). For this wavelength, the atmosphere is optically thin even for upper tropospheric tangent heights and there is no limb radiance maximum at tangent heights (TH) above 10 km even for solar zenith angles approaching 90° for clear-sky conditions. Clouds (or aerosol layers with large optical depths) are identified when the limb radiance profile meets either of the following two conditions:

C1) if a limb radiance maximum exists above the lowest tangent height, the corresponding tangent height is the cloud top height.

C2) if the ~810 nm limb radiance scale height (H_I) is <3.84. The radiance scale height is a measure of the rate of change of radiance (I) between spectra at successive tangent heights

$$H_I = (TH_n - TH_{n+1}) / \ln(I_n / I_{n+1}) \quad (1)$$

with $TH_n < TH_{n+1}$. A 3.84 km scale height threshold is effective for detecting clouds since radiance scale heights of 4 to 7 km occur in the presence of background aerosols in the upper troposphere and lower stratosphere (UT/LS). The value was determined empirically after extensive examination of cloud products generated with different threshold values. If both cloud identification conditions are met during a

scan, the cloud top height is defined to be the higher of the two heights. Both of these conditions are conservative in the sense that minor aerosol layers, including the stratospheric Junge layer, are almost never mistaken for clouds. This point is demonstrated in Fig. 1, which shows the top height of clouds observed in the $\sim 31\,000$ scans processed offline for this work. There are essentially no cloud detections, for example, at northern hemisphere mid-latitudes above 18 km, where the Junge layer (e.g. Hofmann and Rosen, 1981) would be detected if the cloud identification algorithm were sensitive to it.

The second step of the offline retrievals is to verify (and correct) the altitude registration. Newer (and more correct) pointing information is used in this study that was not available when v2.3/2.4 of the operational NO₂ product was generated. We use the tangent height of the simulated ~ 305 nm limb radiance maximum (Sioris et al., 2003), also known as the “knee”, to verify or correct the altitude registration. Often, no correction is required as Odin’s attitude control system is working remarkably well (e.g. within 500 m) and better than expected (Murtagh et al., 2002; Sioris et al., 2003; Haley et al., 2004). The tangent height offset is defined as the difference between the measured and simulated knee TH. The tangent height offset in any limb scan, is corrected if the magnitude of the orbital median TH offset is greater than the standard deviation of the TH offsets during the orbit, based on the approach developed for SCIAMACHY (Sioris et al., 2006).

The ~ 305 nm knee indicates an annual variation in the TH offset, with a departure of ~ 500 m in June relative to the rest of the year, for which the mean offset is -297 m (Fig. 2). It is theorized that the June anomaly is caused by the Odin spacecraft twisting slightly as it cools due to the satellite being eclipsed from the sun by the Earth. Even if the apparent seasonal pointing drift were ignored, this error source translates to $<15\%$ error on the retrieved NO₂ concentration in the tropical upper troposphere (Haley et al., 2004), and thus this is a secondary source of error considering the magnitude of random errors (illustrated below). Assuming the TH offsets determined by the ~ 305 nm knee technique are valid, errors in the NO₂ profile will be even smaller since the TH grid is adjusted prior to the inversion and a June bias will be minimized.

After applying any necessary shift to the altitude registration and limiting the retrieval range based on the cloud top height, each scan is reprocessed with the following modification to the inversion scheme. The inversion scheme was changed to use Chahine’s (1970) relaxation method at each iteration. The advantage of this retrieval scheme is that the vertical resolution of the profiles is ~ 2 km at all retrieved altitudes, and the retrievals are almost completely independent of the first guess. These advantages are important for the current study because lightning-produced enhancements are relatively rare according to OSIRIS but consist of very large concentrations of NO₂ often confined in a narrow ver-

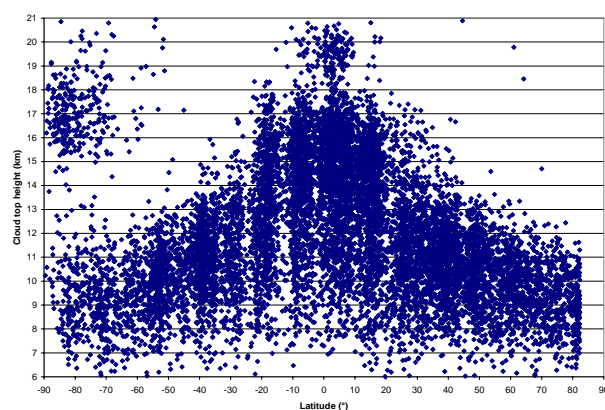


Fig. 1. Cloud top heights observed by OSIRIS from ~ 1100 selected orbits during the period of investigation (27 May 2003–27 May 2005). Orbits are included from each month. Polar stratospheric clouds are observed in austral spring at high latitudes at ~ 17 km.

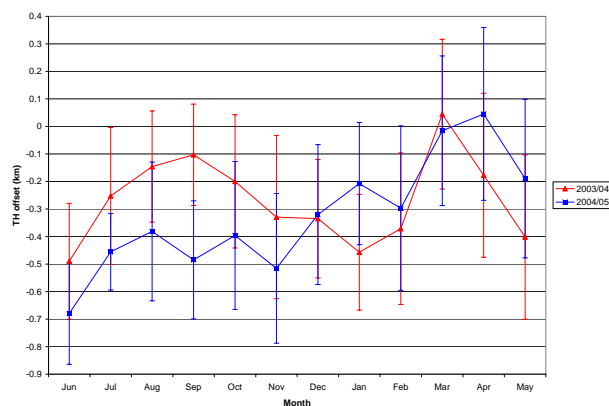


Fig. 2. Monthly mean tangent height offset for OSIRIS as inferred from the ~ 305 nm knee (Sioris et al., 2003). An annual pattern is detected in the two year period of investigation. The error bars show 1 standard deviation about the monthly mean.

tical range (e.g. 2 km), near the bottom of the retrieval range where an optimal estimation approach begins to smooth vertical profiles and rely on a priori information. However, judging from the agreement between the two retrieval schemes (not shown here; see Haley et al., 2004), the reliance on a climatological a priori NO₂ is not as significant an issue as the smoothing of the profiles, and both of these issues are minor. Sioris et al. (2003) showed that the sensitivity of the retrieved NO₂ to the first guess is $<1\%$ below 33 km. The sensitivity to the a priori O₃ profile has been quantified for this work and is $<0.1\%$ for a uniform bias of $+10\%$ in O₃ concentration from the surface to the top of the atmosphere.

We have also added a surface albedo database (Koelemeijer et al., 2003) into the forward (radiative transfer) model, appropriate for clear-sky conditions. Clouds below the field of view are still ignored, leading to $<10\%$ underestimates

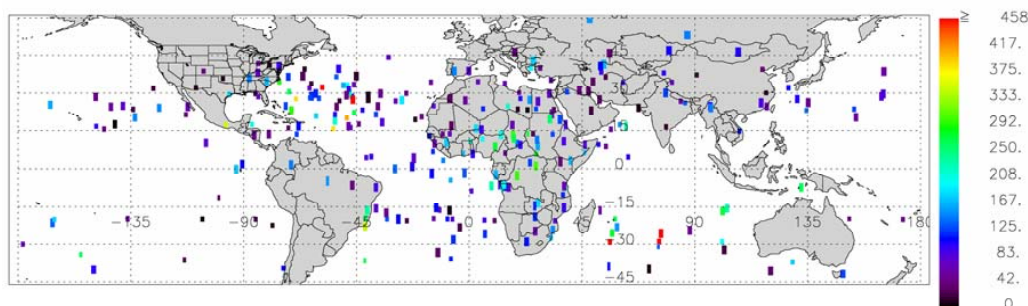


Fig. 3. Map of upper tropospheric NO₂ volume mixing ratio enhancements detected by OSIRIS during the period 27 May 2003 to 27 May 2005. Colour is used to indicate the magnitude of the enhancements in pmol/mol. The longitudinal extent of each OSIRIS spatial pixel has been extended by 0.5° to the east and west of the pixel center for illustrative purposes.

for large solar zenith angles (Sioris et al., 2003) (see also Haley et al., 2004). The retrieval also assumes homogeneous atmospheric composition within an atmospheric layer, ignoring the diurnal gradients that exist between the near and far sides of the limb near twilight (McLinden et al., 2006). In assuming so, we speed up the forward modeling required at each iteration of the inversion at the cost of a minor retrieval error (<10%) in general (McLinden et al., 2006).

The retrieved profiles are examined for NO₂ enhancements. A profile is considered to contain an enhancement if, for the altitude at which an NO₂ enhancement was found in the operational data (see criteria 1–2 above), there is also:

- a an increase relative to the immediately overlying retrieval layer in NO₂ volume mixing ratio (VMR), and
- b an increase in NO₂ absorption optical depth at the closest tangent height underlying the enhanced layer, relative to the immediately overlying tangent height.

Observed VMR enhancements are quantified by taking the difference in VMR as compared to the nearest overlying local minimum in the vertical profile of NO₂ VMR. NO₂ vertical column density (VCD) enhancements are calculated by taking the difference in retrieved NO₂ number density compared to the nearest overlying local minimum in the NO₂ number density profile. These number density enhancements are then integrated over the altitude (z) range exhibiting enhanced values. The VCD enhancements are useful for comparison with nadir viewing instruments (see below).

Some enhancements may be due to aircraft, but it is apparent that aircraft NO_x is only a minor contributor because the spatial distribution of the enhancements (Fig. 3) does not correspond to flight tracks. Another minor source of enhancements is tropopause folds. There are approximately 15 such enhancements observed per year. We have filtered out many of these enhancements that occur primarily at northern mid latitudes (40–50° N in spring) by analyzing the orbital cross-sections of retrieved NO₂ (VMR as a function of latitude and

altitude) to detect anomalously high NO₂ due to a strong descent of stratospheric air. The stratospheric origin of the NO₂ enhancement was confirmed by making use of NCEP 6-h tropopause data (Kalnay et al., 1996). Enhancements also occur in the lower stratosphere during polar spring and are related to renoxification of the polar vortex or dynamical disturbances. These enhancements have been filtered out. We do not fully exclude that some of the upper tropospheric NO₂ enhancements come for surface sources transported upwards within deep convective events.

2.1 Measurement biases

OSIRIS, like all limb scattering instruments, will have a clear sky sampling bias, because limb scans with towering clouds in the field-of-view are omitted from the reprocessing. However, because of the long lifetime of NO_x in the upper troposphere (~1 week, Jaeglé et al., 1998), the NO₂ generated during thunderstorms can be detected after the clouds move away, tens of hours later, thus limiting the severity of this sampling bias. The cloud top heights were shown in Figure 1. It is worth noting that starting abruptly in mid February 2005 and continuing through April 2005, clouds were observed in the intertropical convergence zone (8° N–4° S) with top heights of >18.3 km. The separation between these very high clouds and the usual high clouds observed between 14 and 18 km in the tropics is readily apparent in Fig. 1. These clouds obscure the detection of underlying NO₂ enhancements. The high clouds at high southern latitudes are polar stratospheric clouds observed by OSIRIS in a period near the austral spring equinox (4 September–10 October).

As discussed in the introduction, there is also a spatial coverage bias. For example, the southernmost sunlit (SZA < 90°) latitude observed by OSIRIS on the descending orbital phase (morning) at the start of July, August and September 2004 is 2° S, 5° S, and 16° S, respectively. In October, both hemispheres are covered and then the coverage begins to favour the southern hemisphere until February, after which the northern hemisphere maximal coverage returns

and the annual cycle begins anew. Also, Odin is gradually precessing away from a true dawn/dusk orbit, resulting in an AM/PM bias, with more measurements in the AM, particularly in the tropics.

The month of January 2005 contains few observations as OSIRIS spent most of this month observing the mesosphere in search of polar noctilucent clouds.

3 GEOS-Chem model

We use the GEOS-Chem global 3-D chemical transport model (Bey et al., 2001) for data interpretation. The specific simulation used here, based on GEOS-Chem version 7-02-04 (<http://www-as.harvard.edu/chemistry/trop/geos>), has been previously described by Sauvage et al. (2007). Briefly, the simulation is driven by assimilated meteorological data for the year 2004 from the Goddard Earth Observing System (GEOS-4) at the NASA Global Modeling and Assimilation Office (GMAO). The GEOS-Chem model includes a detailed simulation of tropospheric ozone-NO_x-hydrocarbon chemistry as well as of aerosols and their precursors. The climatological spatial distribution of lightning is scaled locally following Sauvage et al. (2007) to reproduce the climatological seasonal mean lightning flash rates from the Lightning Imaging Sensor and Optical Transient Detector satellite instruments. This spatial scaling has a minor effect (<1.5%) on the globally-averaged NO₂ VMR in the upper troposphere. The local temporal variation of lightning NO_x emissions remains linked to deep convection following the parameterization of Price and Rind (1992) with vertical profiles from Pickering et al. (1998) as implemented by Wang et al. (1998). The midlatitude and global lightning NO_x sources are 1.6 and 6 Tg/year of nitrogen, respectively, following Martin et al. (2006) and Sauvage et al. (2007).

4 Results and discussion

The enhancements in NO₂ VMR detected during the period 27 May 2003 to 27 May 2005 are mapped in Fig. 3. The displayed VMR corresponds to the altitude of the maximum enhancement (i.e. typically 13 km). In all, 283 events are detected producing NO₂ VCD enhancements ranging from 3×10^{13} to 1.6×10^{15} molec/cm² and NO₂ VMR enhancements of 1 to 920 pmol/mol. The smallest observed enhancements might have measurement uncertainties in excess of 100%, but we have not excluded any of the data. The NO₂ retrieval precision (illustrated below) appears to be on the order of 40 pmol/mol at 13 km, which is small relative to the average observed VMR enhancement of ~ 125 pmol/mol, but slightly larger than the background NO₂ concentration in the remote tropical south Pacific Ocean of 25–30 pptv (shown below). For a typical enhancement covering two retrieval layers (or 4 km in altitude), the uncertainty on the VCD integrated

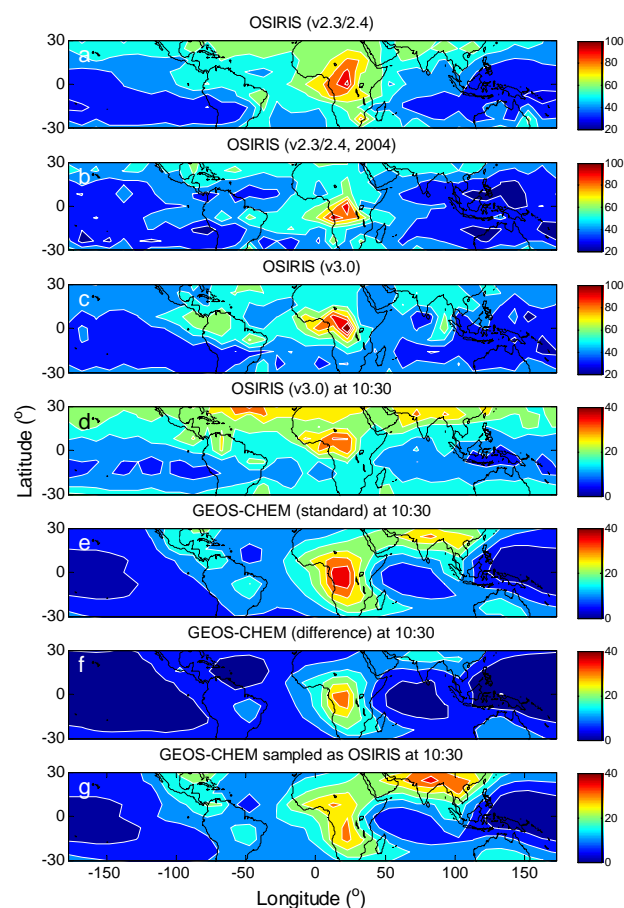


Fig. 4. (a) OSIRIS operational NO₂ VMR (v2.3/2.4) at 12 km, in pmol/mol; AM data only, averaged over all available data and gridded on $8^\circ \times 10^\circ$ (latitude, longitude), (b) same as (a), but for the year 2004, (c) same as (a) but for v3.0, (d) same as (c), but with diurnal scaling to 10:30 LT and with stratospheric points removed by defining the tropopause (see McLinden et al., 2000) as the lowest altitude with 150 nmol/mol of OSIRIS O₃ (v3.0), (e) map of annual mean NO₂ VMR including lightning at $z=12$ km for the year 2000, calculated for 10:30 LT with the GEOS-Chem model. (f) same as (e) except the difference is taken from a model run without lightning to isolate the contribution from lightning, (g) same as (e), except that, an attempt was made to match the spatiotemporal sampling of GEOS-Chem with that of OSIRIS. The monthly mean model data was weighted by the fraction of all OSIRIS data points that occurred in that month in order to make the temporal sampling of GEOS-Chem consistent with that of OSIRIS. The weighting according to the temporal measurement frequency of OSIRIS is performed as a function of latitude.

over the enhanced layers is $\sim 4 \times 10^{13}$ molec/cm². Limb scattering, owing to its long photon paths, is very sensitive to small enhancements in NO₂ in the upper troposphere relative to nadir viewing instruments (discussed below).

Figures 4a–b show the NO₂ VMR at 12 km averaged over all available v2.3/2.4 (2002–2005) and over data only from 2004, respectively. Comparing these two figures, the

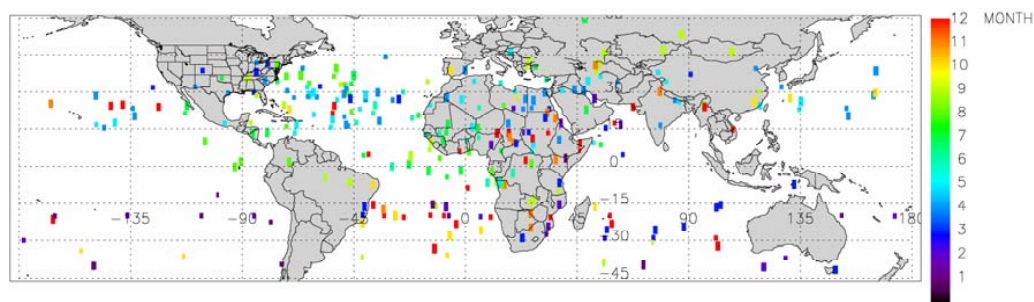


Fig. 5. Location of OSIRIS UT NO₂ enhancements as a function of month over the 2 year period (May 2003–May 2005). December, for example, is the 12th month and thus, observation locations are in red. The longitudinal extent of each OSIRIS spatial pixel has been extended by 0.5° to the east and west of the pixel center for illustrative purposes.

year-to-year variability in the mean NO₂ VMR at 12 km is <20%. Figure 4c shows the NO₂ VMR at 12 km averaged over all available v3.0 data (2002–2006). The v3.0 data suffer from poor statistics in the tropics due to the filtration of “cloudy” cases, whereas v2.3/2.4 data suffer from the retrieval errors caused by the neglect of clouds. However, due to the consistency of the versions as evidenced by the similarity of Figs. 4a and c, it appears that neither problem is major. Figures 4a and c also provides a measure of the upper tropospheric background NO₂ VMR (e.g. 30 pmol/mol over the tropical Pacific Ocean at ~06:30 LT). The OSIRIS observations are scaled to 10:30 LT using the McLinden et al. (2000) photochemical box model (see also Brohede et al., 2007) to match the sampling time of the model simulations (Fig. 4d). This local time was chosen to clearly exclude from the simulated NO₂ field any twilight values (from the winter hemisphere) when NO₂ VMRs are much higher and changing rapidly. The OSIRIS observations (Fig. 4d) provide a similar spatial distribution of NO₂ enhancements to those obtained with the GEOS-Chem 3-dimensional tropospheric chemical transport model (Figs. 4e–f). The spatial correlation coefficient is 0.62. The simulated spatial pattern shown in Figs. 4e–f for $z=12$ km is similar at other upper tropospheric model levels but the NO₂ VMRs are smaller at higher altitudes. Lightning accounts for 60% of the simulated NO₂ at 12 km. Figures 4e–f show that at 12 km, the large majority of the NO₂ over Brazil, and northern India, for example, is from lightning. The maximum of 86% is reached over tropical Africa. Lightning NO₂ is more concentrated over tropical Africa than over Brazil in both the OSIRIS observations and the GEOS-Chem simulation. Lightning flash counts from OTD (Optical Transient Detector) are also higher over tropical Africa than South America (Christian et al., 2003). In South America, the simulated and observed UT NO₂ enhancements lie in eastern Brazil. The ten year mean flash rate over Brazil from LIS and OTD also show more lightning on the eastern half of this country (not shown). Figure 4g shows model data sampled to match to the latitudinally and monthly

dependent sampling pattern of OSIRIS. The sampling of the GEOS-Chem simulated data according to OSIRIS improves the spatial correlation coefficient to 0.67. The latitude range of Fig. 4 is limited to low latitudes since 12 km, the altitude at which enhancements due to lightning are typically largest, frequently lies in the stratosphere at middle and high latitudes.

In order to derive an estimate of the globally-averaged ratio between the observations and the simulations of NO₂ VMR at 12 km, the VMRs in each grid cell are weighted by the cosine of the latitude since the grid cell area decreases in the poleward direction. The weighted average is taken for the latitude region of 30° N–30° S shown in Fig. 4d for OSIRIS and Fig. 4e for GEOS-Chem. The OSIRIS observations suggest larger background NO₂ concentrations in the upper troposphere (by 6 to 7 pmol/mol or 40%), but the difference between the observations and the simulations is within the uncertainty in the lightning source strength derived from other recent global analyses (e.g. Martin et al., 2007; Sauvage et al., 2007). Sampling GEOS-Chem according to OSIRIS increases the simulated mean NO₂ VMR at 12 km, which reduces the bias between OSIRIS and GEOS-Chem by 7%. OSIRIS NO₂ shown in Figure 4d may have a slight high bias partly due to the low cloud albedo assumed in the photochemical modeling of the scaling factor between local times.

The NO₂ enhancements observed by OSIRIS generally occur at 12 to 13 km more frequently than at 10 to 11 km. The mean altitude of the NO₂ number density local maximum is 13.2 ± 1.8 km ($N=283$). This is consistent with the notion that most of the NO₂ is generated by lightning and persisting near the cloud top altitude. Sample profiles are shown below which demonstrate this well-defined peak in NO₂ concentration.

The latitudinal distribution is mostly as expected in the following aspect. In general, the thunderstorms exhibiting weaker vertical development (e.g. to ≤ 13 km) extend latitudinally as far as 45° N and $\sim 40^\circ$ S, but the thunderstorms with stronger vertical development ($z > 13$ km) tend to be

located within 33° of the equator. There is also a hemispheric asymmetry in the frequency of the NO₂ enhancements, as most were observed in the northern hemisphere for the period analyzed, consistent with the GEOS-Chem simulation. The greater abundance of lightning NO_x in the northern hemisphere may relate to the higher fraction of land in this hemisphere as most thunderstorms occur over land.

The overall seasonality of the enhancements is shown in Fig. 5. Lightning NO_x enhancements in the North American outflow region shift from being generally south of 30° N in the boreal spring to ~40° N in midsummer.

As shown in Fig. 3, 55 upper tropospheric (UT) NO₂ enhancements lie in tropical Africa (between 23° S and 23° N). In Fig. 6, we show the latitudinal distribution of enhancements over Africa. Figure 4f shows the contribution of lightning NO₂ in the model simulations extending into Saharan Africa. NO₂ enhancements are also found in the OSIRIS observations in this desert region (Fig. 3). We hypothesize that these enhancements are from advected lightning NO_x since 12 of the 14 enhancements observed over Libya, Egypt and Chad are unaccompanied by coincident LIS lightning observations or any meteorological record of a thunderstorm, whereas globally, the majority of the NO₂ enhancements lie within ±4° of latitude (lat) and longitude (lon) of LIS-observed lightning occurring earlier on the same day or the previous day. Local meteorological data (<http://meteo.infospace.ru/wcarch/html/index.sht>) for the given days usually show that cloud fraction is small and the air at the surface is very dry. Back-trajectory analyses were performed to investigate the origin of the enhancements. We find that most of the lightning flashes which coincided with the back-trajectories in space (within ±4° of lat and lon) and time (within 1 h) occurred over Algeria in the previous 72 h or less.

The most outstanding difference between the simulations and the observations exists in the western North Atlantic near 30° N. There is a trail of NO₂ crossing this marine region in the observations in a latitude band between 27–37° N (Fig. 3). These observations lie at a mean altitude of 11.6±0.9 km, which corresponds very well with the altitude of 12 km for the model simulations. The enhancements in the North Atlantic fall almost evenly into two narrow time periods: late summer (e.g. August) and early spring (late March to early May). Large enhancements from lightning outflow into the western north Atlantic in early August 2004 were observed during the International Consortium for Atmospheric Research on Transport and Transformation (ICARTT) aircraft campaign (Martin et al., 2006; Hudman, et al., 2007, Bertram et al., 2007). The early springtime enhancements correspond to storms with even weaker vertical development than those during late summer. We are uncertain as to the reason the model is not capturing the magnitude of the lightning-produced NO₂ enhancement in the upper troposphere, but a factor of two underestimate was also observed by Martin et al. (2006) at 225 hPa ($z \cong 12$ km) in their analysis of

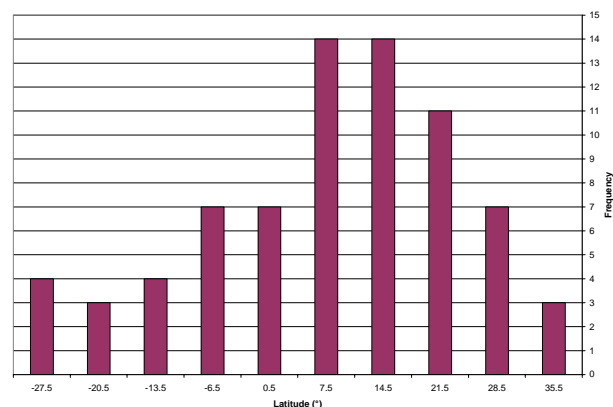


Fig. 6. Histogram of OSIRIS UT NO₂ enhancements detected over Africa over the 2 year period (May 2003–May 2005). The latitude at the midpoint of each bin is labeled on the x-axis.

NO₂ profiles measured by the TD-LIF instrument onboard the DC-8 during ICARTT 2004, even after increasing the northern mid-latitude lightning source to 1.6 Tg/year of nitrogen (see also Hudman et al., 2007). The observed TD-LIF profiles show a greater fraction of NO₂ above 225 hPa than the model. We suspect that the low bias of the model in the North Atlantic (see Martin et al., 2006) and on a global scale (i.e. compare Figs. 4d and g) could be related to the vertical profile of lightning NO_x emissions used in the simulation. Comparison of the mean NO₂ vertical profile from GEOS-Chem and OSIRIS was inconclusive due to insufficient overlap between them. With regard to the magnitude of the observed upper tropospheric column enhancements, they are log-normally distributed with a mode of $\sim 1.5 \times 10^{14}$ molec/cm² (Fig. 7). Given the single-pixel precision of tropospheric NO₂ columns due to spectral fitting is $0.5\text{--}1.5 \times 10^{15}$ molec/cm² (Martin et al., 2006; Wang et al., 2007), it is apparent from Fig. 7 that a large fraction of lightning NO₂ enhancements will be difficult to detect with the current generation of satellite nadir instruments. These nadir-geometry precisions are more than one order of magnitude larger than OSIRIS's precision of 4×10^{13} molec/cm² for an upper tropospheric VCD. Nevertheless, nadir viewing instruments such as GOME have improved our understanding of the contribution of lightning to the tropospheric NO_x budget. Using monthly averaging of GOME NO₂ vertical column densities over a 10° (lat) × 20° (lon) region, increases of 2×10^{14} molec/cm² between winter and summer were linked to lightning (Beirle et al., 2004) in Central Australia. Beirle et al. (2006) found a mean tropospheric NO_x VCD over 9 adjacent GOME pixels during an isolated summer storm in the Gulf of Mexico. Using their stated NO₂ to NO_x ratio, effective for the tropospheric column in the presence of lightning-generated NO_x, the mean NO_x VCD converts to a NO₂ VCD of 2×10^{15} molec/cm². This amount is larger than any of the tropospheric column enhancements above 11.0 km observed

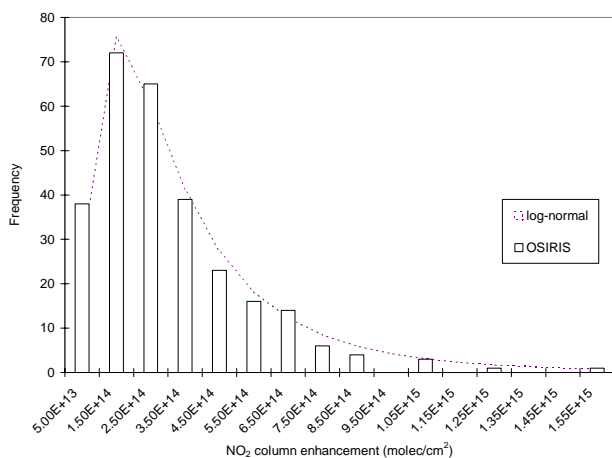


Fig. 7. Distribution of OSIRIS UT NO₂ column enhancements due to lightning is well described ($r^2=0.9754$) by a 3-parameter log-normal distribution. Bin midpoint values are labeled along the x-axis. No effort has been made to scale column enhancements to a single local time.

by OSIRIS (Fig. 7), but is comparable to the magnitude of tropospheric NO₂ column seen by OMI (Levelt et al., 2006) (see below). Boersma et al. (2005) observed a strong relationship between cloud top height and NO₂ column near and above cloud top in annually-averaged GOME data for clouds with top pressures less than 440 hPa. Over ocean, for example, they were able to clearly observe a NO₂ VCD increase from 2.3×10^{14} to 7.5×10^{14} molec/cm² as cloud top height increased from 6.5 km to 12 km. This study also showed good correlations between annually-averaged tropospheric NO₂ VCDs from GOME and lightning NO₂ VCDs from a 3-dimensional chemical transport model (named TM3) in many regions, such as Australia, with GOME observed tropospheric NO₂ VCDs increasing from 2×10^{14} to 9×10^{14} molec/cm² over the range of the TM3-simulated lightning NO₂ VCDs. To summarize these three studies, the detection limit of GOME approaches that of a single limb scattering observation when data are averaged over at least a period of a month or when individual storm studies are limited to cases where lightning enhancements are relatively large. However, the spatial coverage and resolution provided by the current generation of nadir measurements complements the vertical profile information provided by limb scattering.

5 Case studies

As stated above, 283 events, believed to be almost entirely due to lightning-generated NO₂, are found. Details for the ten largest enhancements are given in Table 1. The two largest are studied in detail, as is a third, smaller enhancement detected by three limb-viewing instruments.

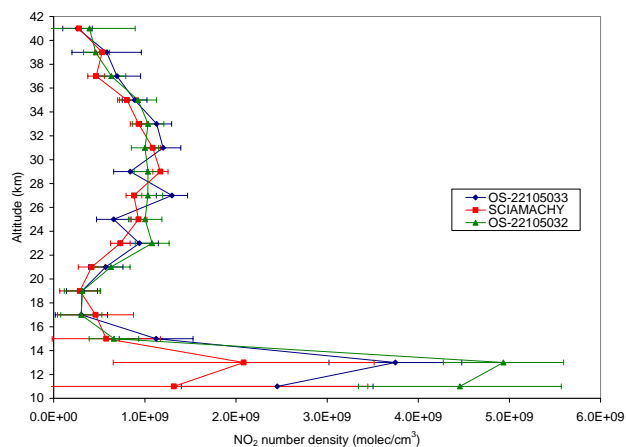


Fig. 8a. Comparison of NO₂ profiles from SCIAMACHY (25.923° S, 76.002° E, SZA=44° AM) and OSIRIS on 15/03/2005 after nearby lightning flashes hours earlier led to large enhancements in NO₂. OSIRIS scans 32 and 33 are at (27.22° S, 76.1° E, SZA=88.09° AM) and (27.949° S, 76.0° E, SZA=88.59° AM), respectively, for TH \approx 13 km. All three profiles have been converted to SZA=88.59° AM to account for diurnal variation using a photochemical model (McLinden et al., 2000; see also Brohede et al., 2007).

5.1 Southern Indian Ocean

On the morning of 15 March 2005, the largest enhancement in the 2-year record was observed by OSIRIS over the southern Indian Ocean. LIS observed a single lightning flash on the previous afternoon (14 March 2005 at 11:21 UTC at 23.94° S, 72.07° E). Other lightning strikes may have occurred but may not have been detected by LIS since, for example, there are large gaps between swaths of successive orbits. OSIRIS detected, at 13 km, NO₂ enhancements of 621 ± 100 and 541 ± 123 pmol/mol in a downscan and successive upscan at (27.2° S, 76.1° E) and (27.9° S, 76.0° E), respectively (Fig. 8a). The OSIRIS spectra recorded at a tangent height of ~ 12 km in each scan are taken 11 s apart, translating to ~ 80 km in the along track direction. Using the HYSPLIT4 dispersion model (Rolph, 2003), we have determined that at 13 km, the plume of NO_x created by the aforementioned lightning flash would have traveled steadily eastward to (23° S, 75.3° E) during the 14 h separating the lightning flash and the OSIRIS observations. This trajectory brings the NO₂ plume closer to the line of sight of OSIRIS. The upper tropospheric NO₂ column ($z > 11.0$ km) observed by SCIAMACHY four hours later (at its local time of $\sim 10:15$) is $(1.2 \pm 0.3) \times 10^{14}$ molec/cm² using the retrieval method of Sioris et al. (2004). SCIAMACHY also provides nadir imagery of tropospheric NO₂ column abundances at high spatial resolution (e.g. 30 km \times 60 km). The corresponding nadir tropospheric columns (see Martin et al., 2006 for further information) are an order of magnitude larger

Table 1. Top ten enhancements in upper tropospheric column NO₂ (in molec/cm²), listed in descending order of column enhancement (see method for details). The difference in NO₂ VMR between the local maximum and the nearest overlying local minimum is “dVMR”.

dd	mm	yyyy	z (km)	lat (°)	lon (°)	AM/ PM	VCD (×10 ¹⁴ molec/cm ²)	VMR (pmol mol ⁻¹)	dVMR (pmol mol ⁻¹)	Remark, LIS info
15	03	2005	13	-26	76	AM	16.4	710	621	S. Indian Ocean; LIS: 11:21 UTC [14/03/2005] (-23.936, 72.074) (see Sect. 5.1)
24	03	2005	11	27	-46	AM	15.1	590	502	Atlantic; (see Sect. 5.2)
15	03	2005	13	-29	76	AM	12.8	633	541	S. Indian Ocean; LIS: 11:21 UTC [14/03/2005] (-23.936, 72.074)
23	03	2005	13	32	-59	PM	10.5	1015	924	Atlantic; (see Sect. 5.2)
12	03	2005	15	-29	56	AM	10.2	901	851	S. Indian Ocean; LIS: 14:03 UTC [11/03/2005] (-24.631, 47.222)
04	06	2004	11	-7	9	AM	10.0	314	231	Atlantic; LIS: 12:17 UTC [03/06/2004] (-1.451, 7.329)
01	04	2005	11	30	-72	PM	8.31	349	259	Atlantic; LIS: 02:09 UTC [01/04/2005] (31.389, -79.425)
04	05	2004	11	-7	13	AM	8.27	312	222	Angola; no coinc. LIS obs.; no lightning or thun- der at ground
16	03	2005	13	-17	101	AM	8.19	301	275	S. Indian Ocean; no LIS lightning, tropical cyclone Willy (see Sect. 5.4)
15	03	2005	13	-16	103	AM	8.15	286	232	S. Indian Ocean; no LIS lightning, tropical cyclone Willy

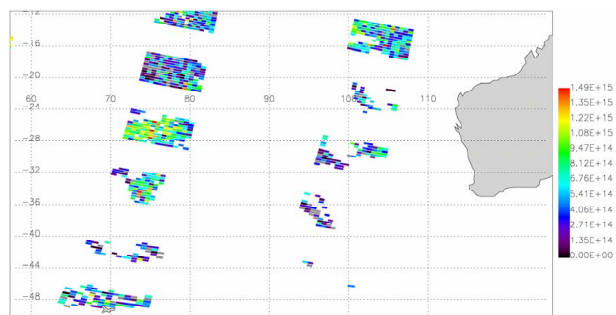


Fig. 8b. SCIAMACHY tropospheric NO₂ column (molec/cm²) map on 15 March 2005, after filtering ground pixels with cloud radiance fraction of >0.5. The NO₂ enhancement stretches over several degrees of longitude (72–79° E) and latitude (25–28° S). Background tropospheric NO₂ column abundances (<10¹⁵ molec/cm²) surround the enhancement to the east, north and south and are also observed in the surrounding nadir states. From coincident SCIAMACHY limb scattering observations, the highest clouds in this region had tops at ~5 km.

(Fig. 8b). This suggests that most of the NO₂ enhancement lies below 11 km in this case. Possible bias in nadir tropospheric column amounts resulting from the sensitivity of the air mass factor to the assumed NO₂ profile shape can only partly explain the magnitude of the difference between the upper tropospheric NO₂ column from limb scattering and the full tropospheric column from nadir. OSIRIS, in successive scans, observed upper tropospheric column enhancements of 1.64×10^{15} and 1.28×10^{15} molec/cm², an order of magnitude larger than SCIAMACHY from limb scattering but, based on photochemical box model calculations (McLinden et al., 2000), a factor of ~4 is attributable to the strong local time dependence of the NO_x partitioning near sunrise (SZA > 80°) and the remaining factor of 2.5 is most likely related to the azimuthal averaging performed in the SCIAMACHY limb data analysis leading to 960 km across-track spatial resolution, judging from the large range in nadir tropospheric VCDs. This is supported by a similar factor of 2.2 which exists between the largest tropospheric VCD (1.72×10^{15} molec/cm²) and the median tropospheric VCD (7.8×10^{14} molec/cm²) over the SCIAMACHY nadir state (with 1σ variability of 3.3×10^{14} molec/cm²). During the four hours between the OSIRIS and SCIAMACHY observations, the lightning NO_x plume transforms slowly into HNO₃. This chemical evolution is not taken into account and could also explain some of the differences between SCIAMACHY and OSIRIS.

This case study demonstrates two advantages of OSIRIS for remote sensing of lightning NO₂: fine across-track resolution and local times near twilight to increase NO₂ absorption signal strength, particularly from the tropopause region.

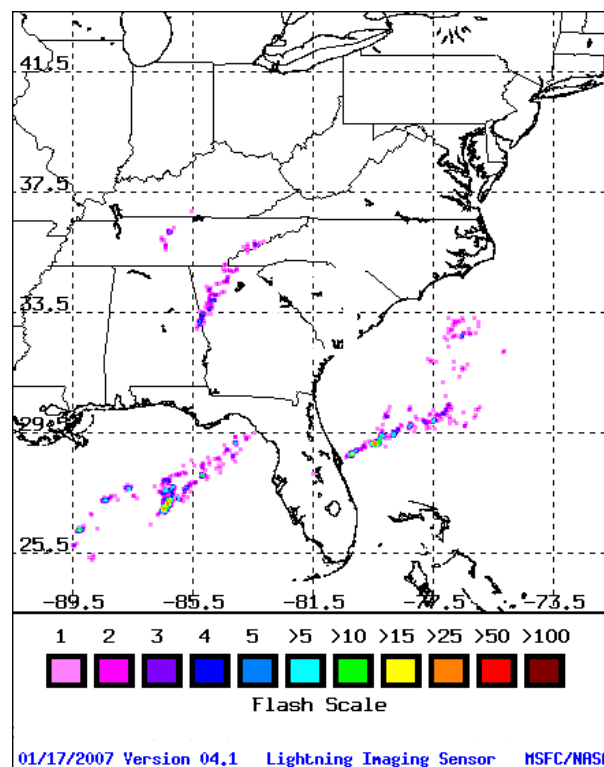


Fig. 9a. Lightning imagery from LIS showing lightning extending out over the Atlantic northeast of Florida at 05:35 UTC on 23 March 2005.

5.2 North Atlantic Ocean

The second largest VCD enhancement during the analyzed time period also occurred in March 2005. NO₂ VMR enhancements of 924 ± 131 , 502 ± 86 , and 293 ± 95 pmol/mol were observed in the western North Atlantic on the afternoon of 23 March 2005 and the following two mornings, respectively. LIS, with only two observing times per day, observed peak flash rates at 05:35 UTC on 23 March 2005 off the Floridian coast as shown in Fig. 9a, but meteorological data (<http://www.wunderground.com>) from Titusville, FL (28.6° N, 80.8° W) indicate a thunderstorm occurred at 00:00 UTC on 23 March 2005. We calculated forward-trajectories using HYSPLIT4 (Fig. 9b) for an altitude of 12.5 km. At this altitude, the trajectory starting at 02:00 UTC on 23 March 2005 is most consistent with OSIRIS NO₂ peak heights on 23, 24 and 25 March 2005 (see below) and with the advection of the NO₂ plume visible in tropospheric column maps (Figs. 9c–d) from OMI (version 2) data (Bucsela et al., 2006). Figure 9e shows that OSIRIS captures the fact that lightning NO_x production, which appears to have originated at ~12.5 km, descended by ~1 km as it flowed across the North Atlantic to the observation geolocation on 24 March 2005. As well, OSIRIS observes the

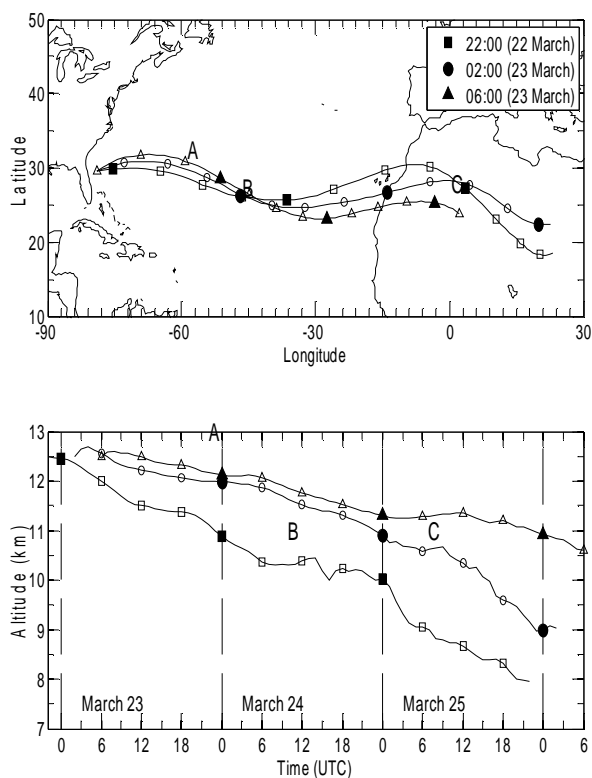


Fig. 9b. 72-h forward trajectories for start geolocation of $z=12.5$ km, 29.5° N, 79° W. Start times of the trajectories are shown in the legend. The bottom panel shows the descent in altitude as the air parcel moves forward in time from off the coast of northern Florida, coincident with the observed thunderstorm. A, B, C indicate the position in time and space of the series of enhancements observed by OSIRIS.

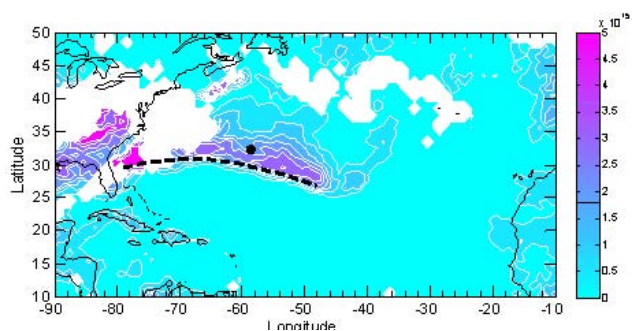


Fig. 9c. Tropospheric column NO₂ (molec/cm²) from OMI on 23 March 2005 showing a plume of NO₂ transported along the trajectory starting at 02:00 UTC on 23 March 2005, also shown in Fig. 9b. The trajectory during the same calendar day (UTC) is shown. The filled black circle represents the location of the OSIRIS profile from the same calendar day (shown below). Cloudy OMI data have been filtered using a cloud fraction threshold of 0.5. The local time of the OMI measurements is approximately 13:30.

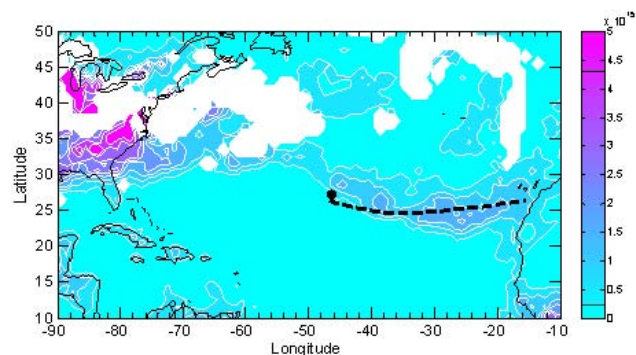


Fig. 9d. Same as (c), except for 24 March 2005. OMI data was not available on 25/03/2005 for the Atlantic region.

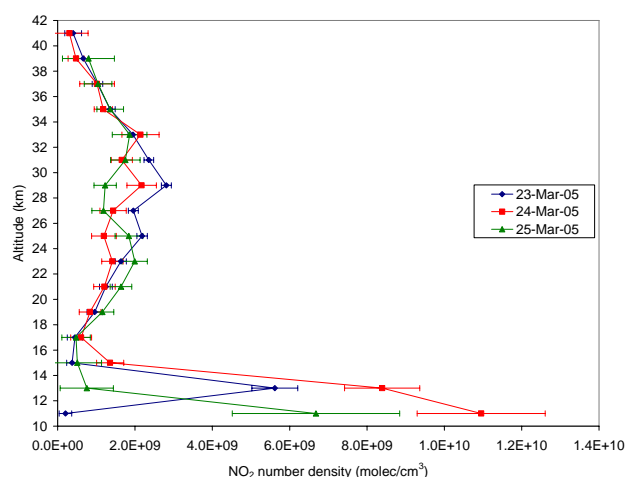


Fig. 9e. NO₂ number density profiles observed by OSIRIS at 32.3° N, 58.7° W on 23/03/2005 (SZA= 89.643° PM), at 27.3° N, 46.4° W on 24 March 2005 (SZA= 80.746° AM), and at 27.7° N, 0.3° E on 25 March 2005 (SZA= 80.563° AM). The profiles on 24–25 March 2005 have been scaled to SZA= 89.643° PM to allow for comparison of the profiles without diurnal differences in NO_x partitioning.

vertical dispersion of the NO₂ from a spike at 12 to 13 km on 23 March 2005 to a broader maximum at ~ 11 km in the 24 March 2005 vertical profile. The continued descent, dispersion and evolution of the elevated-NO_x layer is apparent in the 25 March 2005 profile, which peaks at 11 km, but has smaller NO₂ concentrations there than on the previous day and does not show any significant enhancement at 13 km.

5.3 Tropical South America

We have searched for coincidences with the SCISAT instruments ACE (Atmospheric Chemistry Experiment) and MAESTRO (Measurement of Aerosol Extinction in the Stratosphere and Troposphere by Occultation) (Bernath et al., 2006). A sample coincidence (Fig. 10a) occurred on

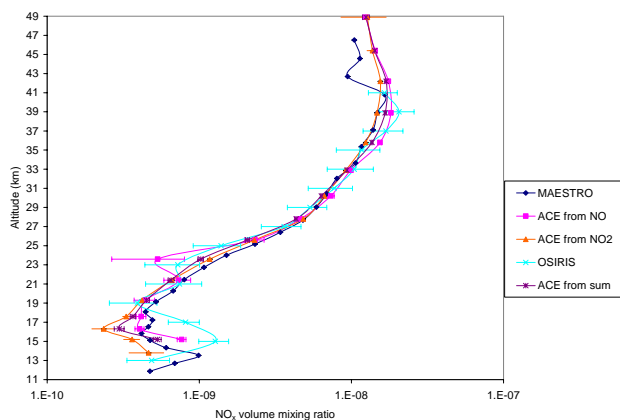


Fig. 10a. Coincident profiles of NO_x inferred from measurements of NO or NO₂ observed by three satellite instruments on 06/08/2004 showing enhanced mixing ratios in the upper troposphere shortly after several nearby lightning strikes in tropical South America. MAESTRO and ACE observed NO₂ while the latter also observed NO at local sunset (3.3° N, 71.7° W). OSIRIS (2° N, 71° N) measured NO₂ just after local sunrise (SZA=85.4°). The NO_x profile has been inferred by appropriately scaling by the NO_x/NO or NO_x/NO₂ ratio from photochemical model calculations (McLinden et al., 2000) with NO_x defined here only as NO + NO₂ + 2 N₂O₅ to account for the diurnal dissociation of N₂O₅. The curve “ACE from sum” is the NO_x calculated by summation and the error bars reflect the quadrature sum of the uncertainties of the three species. For all other curves, uncertainties only reflect the precision of the measured species.

6 August 2004 over tropical South America. LIS had observed several lightning flashes on 5 August 2004 just north of the equator at a longitude of 71° W (Fig. 10b). OSIRIS detected a coincident NO₂ enhancement at 15 km. The LIS flash observations were also coincident with MAESTRO, which observed an NO₂ local maximum at 13.53 km, and ACE, which observed a local maximum in NO₂ volume mixing ratio at 13.8 km, and a local maximum in NO at the lowest point in that profile at 15.2 km. The OSIRIS NO₂ profile has been converted to local sunset with the photochemical model, and all of the instruments are consistent in terms of the inferred NO_x. In the upper troposphere, all of the instruments paint a consistent picture of a NO_x maximum at 14–15 km. Prior to inferring NO_x, we have corrected for the large diurnal effect error in the occultation measurements (Brohede et al., 2007), particularly for NO. There are a few other cases of coincident enhancements in NO, NO₂, and/or HNO₃ between ACE, MAESTRO and OSIRIS. Thus, it appears that the SCISAT instruments can also assist in the global measurement of lightning NO_x and NO_y from space.

5.4 Tropical cyclones

On successive days in mid-March 2005, OSIRIS observed the 9th and 10th largest enhancements in upper tropospheric

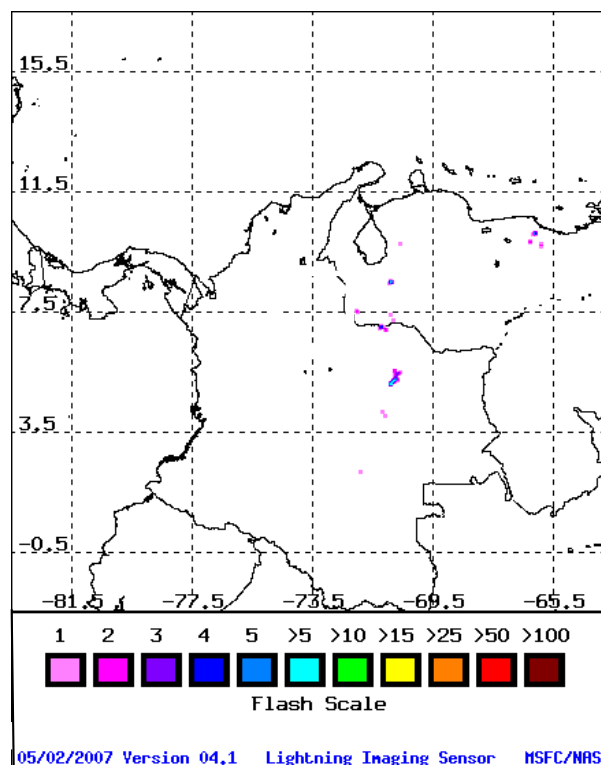


Fig. 10b. Map of lightning flashes from LIS over Colombia on 5 August 2004 between 06:13 and 08:01 UTC.

NO₂ in the 2-year period (see Table 1). These enhancements were located over the south Indian Ocean and were generated by tropical cyclone 23S (Category 2), also known as Willy. Hurricane Ivan also appears to have been responsible for an enhancement of UT NO₂ observed on 19 September 2004. However, these were the only two tropical cyclones (see <http://weather.unisys.com/hurricane/>) observed by OSIRIS to generate significant lightning NO₂ in the 2-year period, indicating that hurricanes generally produce very little lightning compared to other storms, consistent with the work of Molinari et al. (1994).

6 Summary, conclusions and future work

We have searched two years (May 2003–May 2005) of OSIRIS (Optical Spectrograph and Infrared Imager System) operational nitrogen dioxide data (version 2.3/2.4) to find large enhancements in the observations by comparing concentrations with those predicted by a photochemical model and by identifying local maxima in NO₂ volume mixing ratio. We have reanalyzed these cases with an improved algorithm, which retrieves only down to cloud top height if clouds are detected above 10 km.

We find that enhancements in upper tropospheric NO₂ are readily observed by OSIRIS. Most of these enhancements are

found in locations near where lightning has occurred on the previous day or earlier on the same day. LIS and hourly meteorological reports from surface sites were used to locate the lightning in space and time. Many enhancements are seen by OSIRIS in consecutive limb scans or after 12 h in the downwind direction, demonstrating both the self-consistency and valuable spatio-temporal coverage of the OSIRIS observations. The SCIAMACHY and OMI tropospheric NO₂ column maps reveal the large spatial extent (>900 km) of enhanced NO_x generated from thunderstorms, such as in a case over the southern Indian Ocean.

The simulation of lightning NO_x in the upper troposphere with the GEOS-Chem chemical transport model is consistent with the enhancements observed by OSIRIS in terms of the overall spatial pattern of lightning-induced hotspots, and in the advection of lightning NO_x (e.g. across northeastern Africa from source regions such as western and central Africa). Several possible sources of high bias in the OSIRIS NO₂ observations at 12 km were removed for the purpose of comparing with the GEOS-Chem simulations. We accounted for the strong diurnal variation in the NO₂ data set of OSIRIS (which often measures near twilight) by converting all profiles to mid-morning. The sampling bias toward summer hemisphere data was taken into account as well. Finally, stratospheric NO₂ was filtered from the observations. Nevertheless, the OSIRIS background NO₂ VMR at 12 km remains, on average, 6 to 7 pmol/mol higher than the simulations. Thus, OSIRIS observations at 12 km could suggest a 40% increase in the global lightning source strength to the upper troposphere in the GEOS-Chem simulations. MAESTRO observations of lightning-generated NO₂ may assist in characterizing the assumed profile shape, given the ~1 km vertical resolution of this instrument.

Even though most lightning occurs over land (Christian et al., 2003), NO₂ enhancements frequently appear over the ocean due to transport and the long lifetime of NO_x in the upper troposphere. In the northern Atlantic Ocean, a band of enhanced NO₂ is observed. It appears to be a result of outflow from the southeast US, starting in spring at ~25° N and moving to higher latitudes in boreal summer. In contrast, fewer upper tropospheric NO₂ enhancements are found in the Pacific and Indian Oceans and lower baseline concentrations of NO₂ are observed there, consistent with the simulations. Coincident profile measurements through the entire troposphere of trace gases with sources primarily at the surface, such as CO, would reduce uncertainty about the role of convective transport.

Acknowledgements. The authors gratefully acknowledge the NOAA Air Resources Laboratory (ARL) for the provision of the HYSPLIT transport and dispersion model and the READY website (<http://www.arl.noaa.gov/ready.html>) used in this publication. NCEP reanalysis data are provided by the NOAA/OAR/ESRL PSD, Boulder, Colorado, USA, from their website at <http://www.cdc.noaa.gov/>. We also thank the LIS and OMI teams for their publicly available data. This work and the ACE mission are supported

by the Canadian Space Agency and Natural Science and Engineering Research Council of Canada. Work at Dalhousie University was supported by the Canadian Foundation for Climate and

Atmospheric Sciences through the Stratospheric Processes and their Role in Climate Program.

Edited by: R. Cohen

References

- Beirle, S., Spichtinger, N., Stohl, A., Cummins, K. L., Turner, T., Boccippio, D., Cooper, O. R., Wenig, M., Grzegorski, M., Platt, U., and Wagner, T.: Estimating the NO_x produced by lightning from GOME and NLDN data: A case study in the Gulf of Mexico, *Atmos. Chem. Phys.*, 6, 1075–1089, 2006, <http://www.atmos-chem-phys.net/6/1075/2006/>.
- Beirle, S., Platt, U., Wenig, M., and Wagner, T.: NO_x production by lightning estimated with GOME, *Adv. Space Res.*, 34, 793–797, 2004.
- Bernath, P. F., McElroy, C. T., Abrams, M. C., et al.: Atmospheric Chemistry Experiment (ACE): Mission overview, *Geophys. Res. Lett.*, 32, L15S01, doi:10.1029/2005GL022386, 2005.
- Bertram, T. H., Perring, A. E., Wooldridge, P. J., et al.: Direct measurements of the convective recycling of the upper troposphere, *Science*, 315, 816–820, 2007.
- Bey, I., Jacob, D. J., Yantosca, R. M., Logan, J. A., Field, B., Fiore, A. M., Li, Q., Liu, H., Mickley, L. J., and Schultz, M.: Global modeling of tropospheric chemistry with assimilated meteorology: Model description and evaluation, *J. Geophys. Res.*, 106, 23 073–23 096, 2001.
- Bovensmann, H., Burrows, J. P., Buchwitz, M., Frerick, J., Noël, S., Rozanov, V. V., Chance, K. V., and Goede, A. P. H.: SCIAMACHY: Mission objectives and measurement modes, *J. Atmos. Sci.*, 56, 127–150, 1999.
- Brohede, S. M., Haley, C. S., McLinden, C. A., et al.: Validation of Odin/OSIRIS stratospheric NO₂ profiles, *J. Geophys. Res.*, 112, D07310, doi:10.1029/2006JD007586, 2007.
- Bucsel, E. J., Celarier, E. A., Wenig, M. O., Gleason, J. F., Veefkind, J. P., Boersma, K. F., and Brinksma, E. J.: Algorithm for NO₂ vertical column retrieval from the Ozone Monitoring Instrument, *IEEE Trans. Geosci. Remote Sens.*, 44, 1245–1258, 2006.
- Chahine, M. T.: Inverse problems in radiative transfer: Determination of atmospheric parameters, *J. Atmos. Sci.*, 27, 960–967, 1970.
- Christian, H. J., Blakeslee, R. J., Boccippio, D. J., et al.: Global frequency and distribution of lightning as observed from space by the Optical Transient Detector, *J. Geophys. Res.*, 108(D1), 4005, doi:10.1029/2002JD002347, 2003.
- Funke, B., López-Puertas, M., von Clarmann, T., et al.: Retrieval of stratospheric NO_x from 5.3 and 6.2 mm nonlocal thermodynamic equilibrium emissions measured by Michelson Interferometer for Passive Atmospheric Sounding (MIPAS) on Envisat, *J. Geophys. Res.*, 110, D09302, doi:10.1029/2004JD005225, 2005.
- Haley, C. S., Brohede, S. M., Sioris, C. E., Griffioen, E., Murtagh, D. P., McDade, I. C., Eriksson, P., Llewellyn, E. J., Bazureau, A., and Goutail, F.: Retrieval of stratospheric O₃ and NO₂ pro-

- files from Odin Optical Spectrograph and Infrared Imager System (OSIRIS) limb-scattered sunlight measurements, *J. Geophys. Res.*, 109, D16303, doi:10.1029/2004JD004588, 2004.
- Heitzler, J. R.: The future of the South Atlantic anomaly and implications for radiation damage in space, *J. Atmos. Solar-Terr. Phys.*, 64, 1701–1708, 2002.
- Hofmann, D. J. and Rosen, J. M.: On the background stratospheric aerosol layer, *J. Atmos. Sci.*, 38, 168–181, 1981.
- Hudman, R. C., Jacob, D. J., Turquety, S., et al.: Surface and lightning sources of nitrogen oxides over the United States: magnitudes, chemical evolution, and outflow, *J. Geophys. Res.*, 112, D12S05, doi:10.1029/2006JD007912, 2007.
- Intergovernmental Panel on Climate Change, *Climate change 2001: The scientific basis*, 881 pp., Cambridge University Press, Cambridge, UK, 2001.
- Jaeglé, L., Jacob, D. J., Wang, Y., Weinheimer, A. J., Ridley, B. A., Campos, T. L., Sachse, G. W., and Hagen, D. E.: Sources and chemistry of NO_x in the upper troposphere over the United States, *Geophys. Res. Lett.*, 25, 1705–1708, 1998.
- Kalnay, E., Kanamitsu, M., Kistler, R., et al.: The NCEP/NCAR 40-year reanalysis project, *Bull. Amer. Meteorol. Soc.*, 77, 437–470, 1996.
- Koelemeijer, R. B. A., de Haan, J. F., and Stammes, P.: A database of spectral surface reflectivity in the range 335–772 nm derived from 5.5 years of GOME observations, *J. Geophys. Res.*, 108(D2), 4070, doi:10.1029/2002JD002429, 2003.
- Lamarque, J. F., Brasseur, G. P., Hess, P. G., and Mueller, J. F.: Three-dimensional study of the relative contributions of the different nitrogen sources in the troposphere, *J. Geophys. Res.*, 101, 22 955–22 968, 2006.
- Levelt, P. F., van den Oord, G. H. J., Dobber, M. R., Mälkki, A., Visser, H., de Vries, J., Stammes, P., Lundell, J., and Saari, H.: The Ozone Monitoring Instrument, *IEEE Trans. Geosci. Remote Sens.*, 44, 1093–1101, 2006.
- Llewellyn, E. J., Lloyd, N. D., Degenstein, D. A., et al.: The OSIRIS instrument on the Odin satellite, *Can. J. Phys.*, 82, 411–422, 2004.
- Martin, R. V., Sauvage, B., Folkins, I., Sioris, C. E., Boone, C., Bernath, P., and Ziemke, J.: Space-based constraints on the production of nitric oxide by lightning, *J. Geophys. Res.*, 112, D09309, doi:10.1029/2006JD007831, 2007.
- Martin, R. V., Sioris, C. E., Chance, K., Ryerson, T. B., Bertram, T. H., Wooldridge, P. J., Cohen, R. C., Neuman, J. A., Swanson, A. L., and Flocke, F. M.: Evaluation of space-based constraints on global nitrogen oxide emissions with regional aircraft measurements over and downwind of eastern North America, *J. Geophys. Res.*, 111, D15308, doi:10.1029/2005JD006680, 2006.
- McLinden, C. A., Olsen, S. C., Hannegan, B. J., Wild, O., Prather, M. J., and Sundet, J.: Stratospheric Ozone in 3-D Models: A simple chemistry and the cross-tropopause flux, *J. Geophys. Res.*, 105, 14 653–14 665, 2000.
- McLinden, C. A., Haley, C. S., and Sioris, C. E.: Diurnal effects in limb scatter observations, *J. Geophys. Res.*, 111, D14302, doi:10.1029/2005JD006628, 2006.
- Molinari, J., Moore, P. K., Idone, V. P., Henderson, R. W., and Saljoughy, A. B.: Cloud-to-ground lightning in Hurricane Andrew, *J. Geophys. Res.*, 99(D8), 16 665–16 676, 1994.
- Murtagh, D., Frisk, U., Merino, F., et al.: An overview of the Odin atmospheric mission, *Can. J. Phys.*, 80, 309–319, 2002.
- Nesbitt, S. W., Zhang, R., and Orville, R. E.: Seasonal and global NO_x production by lightning estimated from the Optical Transient Detector (OTD), *Tellus*, 52B, 1206–1215, 2000.
- Pickering, K. E., Wang, Y. S., Tao, W. K., Price, C., and Muller, J. F.: Vertical distributions of lightning NO_x for use in regional and global chemical transport models, *J. Geophys. Res.*, 103(D23), 31 203–31 216, 1998.
- Price, C. and Rind, D.: A simple lightning parameterization for calculating global lightning distributions, *J. Geophys. Res.*, 97, 9919–9933, 1992.
- Price, C., Penner, J., and Prather, M.: NO_x from lightning 1. Global distribution based on lightning physics, *J. Geophys. Res.*, 102, 5929–5941, 1997.
- Rolph, G. D.: Real-time Environmental Applications and Display sYstem (READY) Website (<http://www.arl.noaa.gov/ready/hysplit4.html>). NOAA Air Resources Laboratory, Silver Spring, MD, 2003.
- Sauvage, B., Martin, R. V., van Donkelaar, A., Liu, X., Chance, K., Jaeglé, L., Palmer, P. I., Wu, S., and Fu, T.-M.: Remote sensed and in situ constraints on processes affecting tropical tropospheric ozone, *Atmos. Chem. Phys.*, 7, 815–838, 2007, <http://www.atmos-chem-phys.net/7/815/2007/>.
- Schumann, U. and Huntrieser, H.: The global lightning-induced nitrogen oxides source, *Atmos. Chem. Phys. Discuss.*, 7, 2623–2818, 2007, <http://www.atmos-chem-phys-discuss.net/7/2623/2007/>.
- Sioris, C. E., Haley, C. S., McLinden, C. A., et al.: Stratospheric profiles of nitrogen dioxide observed by Optical Spectrograph and Infrared Imager System on the Odin satellite, *J. Geophys. Res.*, 108(D7), 4215, doi:10.1029/2002JD002672, 2003.
- Sioris, C. E., Kurosu, T. P., Martin, R. V., and Chance, K.: Stratospheric and tropospheric NO₂ observed by SCIAMACHY: First results, *Adv. Space Res.*, 34(4), 780–785, 2004.
- Sioris, C. E., Kovalenko, L. J., McLinden, C. A., et al.: Latitudinal and vertical distribution of bromine monoxide in the lower stratosphere from SCIAMACHY limb scattering measurements, *J. Geophys. Res.*, 111, D14301, doi:10.1029/2005JD006479, 2006.
- Wang, Y., Jacob, D. J., and Logan, J. A.: Global simulation of tropospheric O₃-NO_x-hydrocarbon chemistry, 1. Model formulation, *J. Geophys. Res.*, 103, 10 713–10 726, 1998.
- Wang, Y., McElroy, M. B., Boersma, K. F., Eskes, H. J., and Veefkind, J. P.: Traffic restrictions associated with the Sino-African summit: Reductions of NO_x detected from space, *Geophys. Res. Lett.*, 34, L08814, doi:10.1029/2007GL029326, 2007.
- World Meteorological Organization, *Scientific Assessment of Ozone Depletion: 1998*, Geneva, Switzerland, 1999.